# Design, Fabrication and Parametric Study of Bulk Current Injection Probe and Its Calibration Fixture

Issa M. Mashriki[1], S.M.J. Razavi[2], S.H.M. Armaki[2]

*High Institute for Applied Science and Technology, Syria, Damascus.[1]*
*Faculty of Electrical & Computer Engineering, Malek Ashter University of Technology, Iran, Tehran.[2]*
Corresponding Author: razavismj@mut.ac.ir

***Abstract-*** **In this paper, the fabrication of a bulk current injection (BCI) probe using two different ferrite materials and a wideband rounded-shield calibration fixture or jig used to calibrate BCI probe are presented. Some optimization ideas are also investigated to increase their performance. The effect of change in various parameters such as slot distance, probe's shield to probe's core spacing and the inner surface of probe's shield on the probe high frequency performance and insertion loss (IL) have been studied. Results show that increasing the slot distance improves the high frequency response of the probe and increasing the probe's shield to probe's core spacing would affect negatively on measured IL and decreasing the inner surface of probe's shield improves the probe working bandwidth.**

***Index Terms-*** Bulk current injection (BCI), calibration fixture (CF or JIG), electromagnetic Compatibility (EMC), optimization, parametric study.

## I. INTRODUCTION

Bulk current injection probe (BCI) is a conducted-susceptibility (CS) test device based on the injection of common-mode (CM) noise currents in bundles of wires and cables. It is widely used in electromagnetic compatibility (EMC) test procedures. BCI-based techniques have progressively gained the attention of several international standards, because they permit interference testing at the early design stage without making any change in the device connections, and provide a low-cost way to verify the immunity against radiated interference when compared with the classical test procedures in fully-anechoic chamber (FAC). These advantages made BCI techniques accepted by all regulatory standards [1-6].

Each BCI probe is provided, from its manufacturer, with a calibration fixture(CF). The purpose of calibration is to determine the power level required from the signal generator to get a predefined
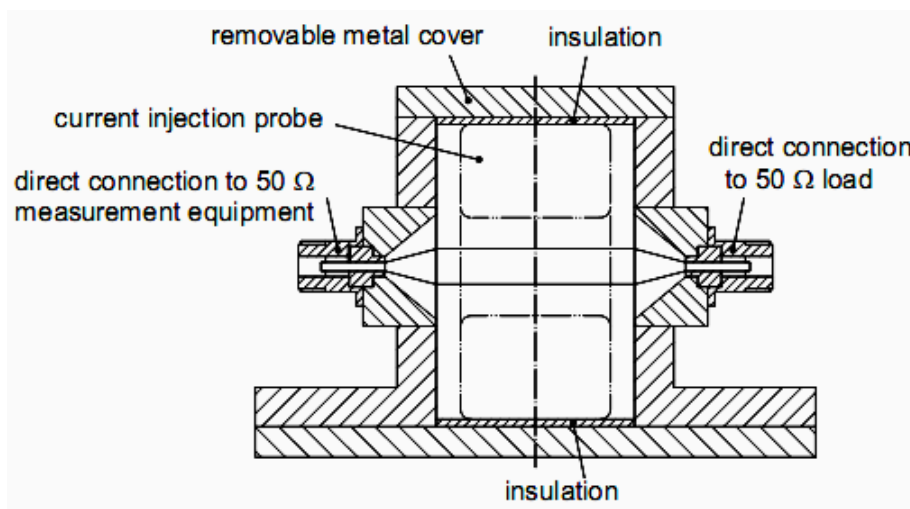
Fig. 1. Typical configuration of calibration fixture [4].

current level on a 50Ω adapted load. The test current curve, depending on the frequency, is defined in the EMC specification associated with the device under test. The outlines of a typical calibration fixture is illustrated in the front sectional view of Fig. 1 It consists from  an inner copper (Cu) rod welded from each side to the inner pin of a 50Ω N-type pass-through connector via a conical part to adapt the cross section of the copper rod to that of connector pin.The outer shield is made flat, from the left and right sides the jig shield is connected to the shield of  N-type connector via a conical part. The tapered region between the shield and copper rod cones is filled with Teflon (PTFE). The clamping window, into which the BCI probe is inserted, agrees with the probe size and configuration, so that, no electrical connection exists between the jig shield and the probe's one.

In the first part of this article, the design and construction of BCI probe is reported. In the second part, optimization and construction of its calibration fixture are presented. In the last part, the parametric study of both structures is discussed.

## II.   DESIGN AND CONSTRUCTION OF BCI PROBE

BCI probe is a wide band power transformer, with mostly one turn primary coil wound around a toroidal ferrite core. Fig. 2 illustrates a radial cross sectional view of a typical BCI probe, the terminals of primary coil are connected to a N-type 50Ω RF-connector, one terminal is attached to the inner pin while the other one is connected to the external shield. The probe is shielded using two identical aluminum frames connected together with the outer shield of the connector from the outer side of the probe, and separated by a small slot from the inner one.

When the BCI-probe is not clamped on the wire under test, the shield is seen by the primary as a secondary coil with one turn loaded by the slot capacitance, and a capacitance forms between the
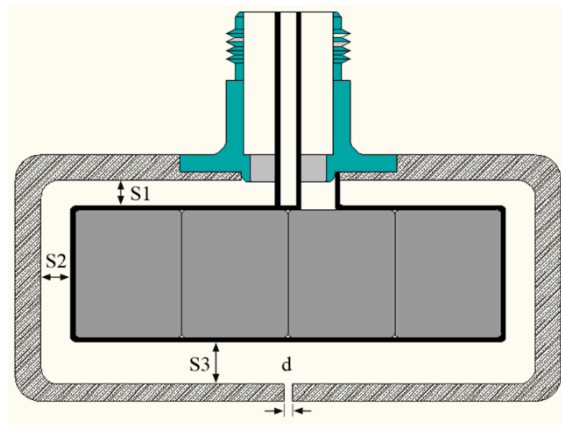
Fig. 2. Radial cross-section of a general type BCI probe with its input connector and layout parameters.



Fig. 3. Materials used in constructing the BCI-probe.



(a)                                                        (b)

Fig. 4. (a) Assembling four core together (b) The way of fixing the core in the shield.

shield and the primary turn. The main materials used in fabricating the BCI-probe are shown in Fig. 3, two layers of copper sheets with width 10 mm were used in implementing the single turn coil. The core is a result of assembling four toroidal cores together as shown in Fig. 4(a). The way of fixing the toroidal core in the shield is shown in Fig. 4(b), a small parts of a spongy material were used to separate the core from the shield. When the probe is clamped onto its jig, a three port network would
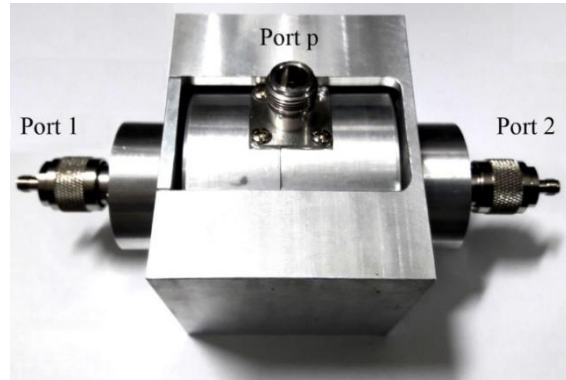
Fig. 5. The network ports definition for test

Table 1.  Cross-sectional view of toroidal core and characteristic parameters of used cores.

| | Core | Model | $\mu_i$ | A(mm) | B(mm) | C(mm) | $\rho(g/cm^3)$ |
|---|---|---|---|---|---|---|---|
|  | Fair-Rite (#61) | 5961003801 | 125 | 61 | 35.55 | 12.7 | 30 |
| | WURTH (#4W620) | 710-74270097 | 620 | 61 | 35.5 | 12.7 | 27 |

result, the names chosen for these ports are shown in Fig. 5, and the studied or altered layout parameters are illustrated in Fig. 2. Preliminarily, these parameters have the following values: (S1 = 2.5 mm, S2 = 4.1 mm, S3 = 5.2 mm and d = 0.5 mm). Cross-sectional view of used toroidal cores with their characteristic parameters listed in Table 1. To achieve the needed tests using VNA model HP8510, the device is provided by a SMA-to-N adapter at each port to allow the use of coaxial cables equipped with SMA connectors. The available minimum testing frequency of used VNA is 45MHz, but since our aim is to improve the HF performance it would be sufficient. The VNA is calibrated in the frequency range 45-1100 MHz, and measurements are carried out at this frequency interval.

The definition of probe's IL and transfer impedance and the setup used for measuring it was discussed in [4]. According to it, the measure of the magnitude of scattering parameter $S_{1p}$ in dB, when port 2 is connected to a matched load, represents the IL. The result of measuring the IL for the two prototypes is shown in Fig. 6, it shows that Wurth prototype has a better IL than Fair-Rite prototype at high frequencies.

 The transfer impedance is given from measured $S_{p1}$ using the formula (1), with port 2 is connected to a matched load.

$$Z_T|_{dB\Omega} = 34 + 20log|S_{p1}| \tag{1}$$

 Measured transfer impedance for the proposed prototypes is shown in Fig. 7, it shows that the transfer impedance of Wurth prototype is higher than that for the Fair-Rite at high frequencies.
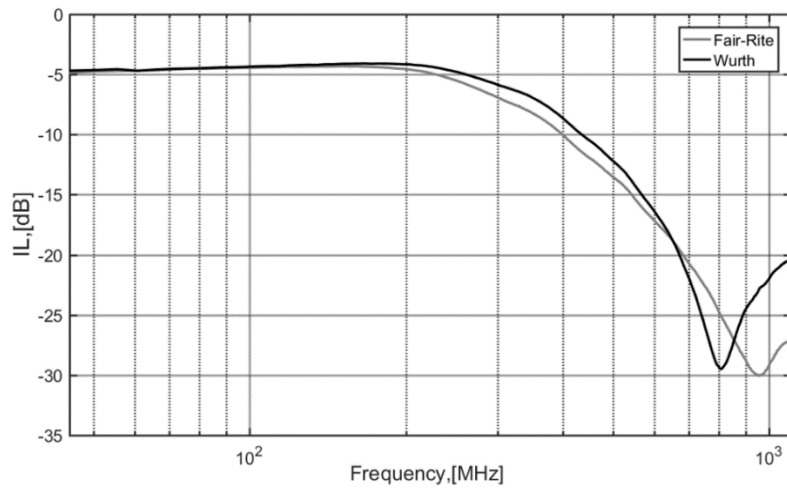
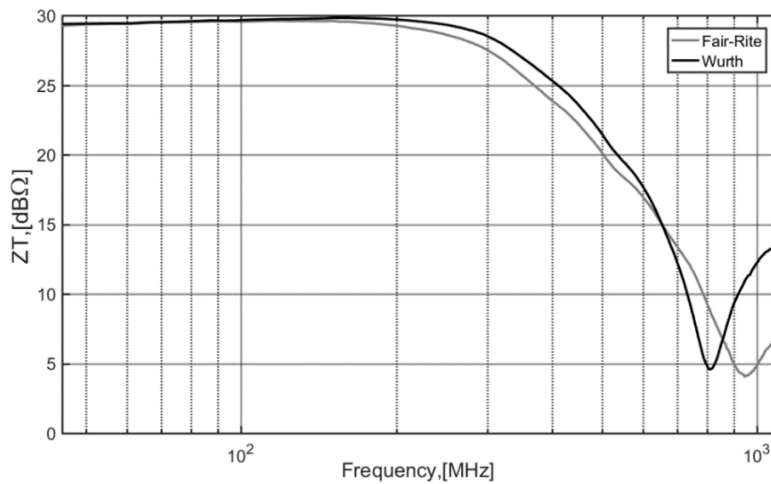Fig. 6.  Measured IL of Wurth prototype versus Fair-Rite.



Fig. 7.  Measured transfer impedance of Wurth prototype versus Fair-Rite.

## III. OPTIMIZATION AND CONSTRUCTION OF CALIBRATION JIG

The calibration fixture or jig is a main part of the test equipment required by any BCI test procedure specifications, therefore, each BCI probe is associated by its manufacturer with a compatible band jig. It allows the user to quickly and easily calibrate the injection probe prior to performing compliance testing. Calibrating is used to establish the forward power into the injection probe needed to develop the specified currents in the system under test [7]. Other applications of the jig are to measure the injection probes insertion loss, and to measure the transfer impedance of current probes ([8] and [9]).

### A. Design

A circuit model for the calibration fixture model FCC-BCICF-1 with bandwidth up to 400 MHz was derived in [10], and an electromagnetic (EM) model was derived in [11] for the BCI probe model FCC-F130A in order to integrate it with its corresponding fixture FCC-BCICF-1. All related articles,
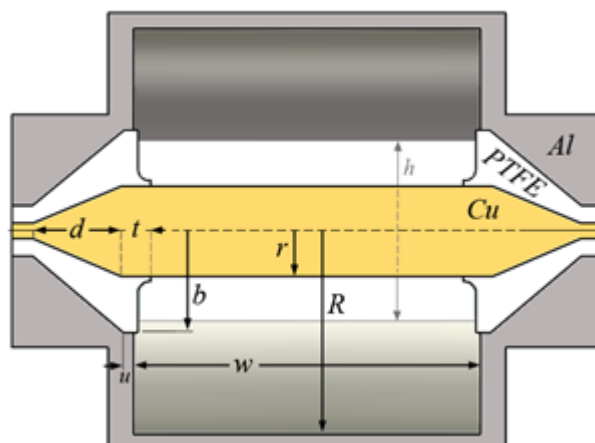
Fig. 8. Front sectional view of the calibration fixture with its layout parameters.

Table 2. The jig dimensional parameters in [mm]

| r | R | w | b | d | u | T | h |
|---|---|---|---|---|---|---|---|
| 9 | 40 | 69 | 20 | 18 | 2 | 5.5 | 36 |

concentrate on modeling the jig to achieve a specific application or test setup. The work done here manipulate the device from its design and performance point of view. In this article, a new jig with modified design is fabricated and simulated, the jig is mainly characterized by a rounded (instead of flat) shield.

The construction of proposed calibration fixture with its layout parameters are illustrated in the front sectional view of Fig. 8. It consists of an inner copper (Cu) rod of radius r and length (w+2u) welded from each side to the inner pin conductor of a 50Ω N-type pass-through connector (not shown) via a conical part of length d to adapt the cross section of the copper rod to that of the connector pin.

The outer shield is made from aluminum (Al). In the clamping region, the shied is of radius R  and width w with aperture of height h from the back and front side. From the left and right sides the jig shield is connected to the shield of N-type connector via a cylindrical section of radius b and width u followed by a tapered section of width d. The tapered regions between the shield and copper rod cones are filled with Teflon (PTFE) and extends about 1mm into the probe's clamping region to avoid any electrical contact between the jig shield and the probe's one. The main layout parameters, in [mm], used in implementing the proposed device are listed in Table 2.

*B. Optimization*

The aim of optimization is to improve the band frequency of the proposed jig to be usable for calibrating the same size of BCI probe with wider band, which means to conserve the clamping window.

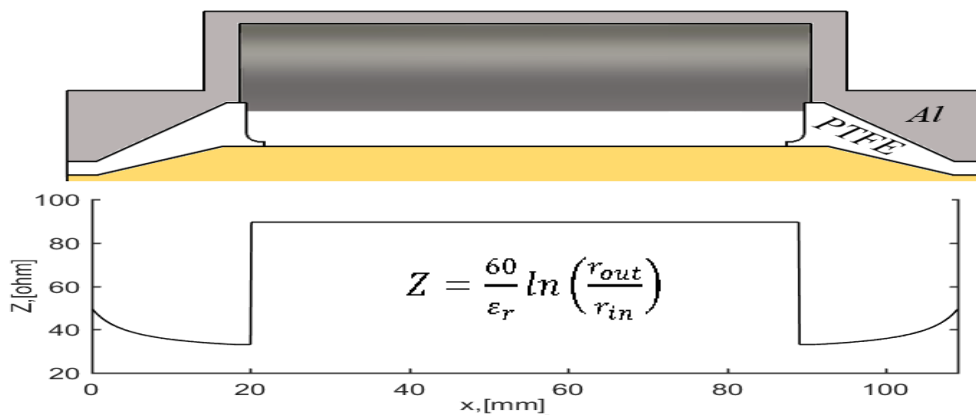$$Z = \frac{60}{\varepsilon_r} ln\left(\frac{r_{out}}{r_{in}}\right)$$

Fig. 9. Characteristic impedance distribution within the full width of the jig.
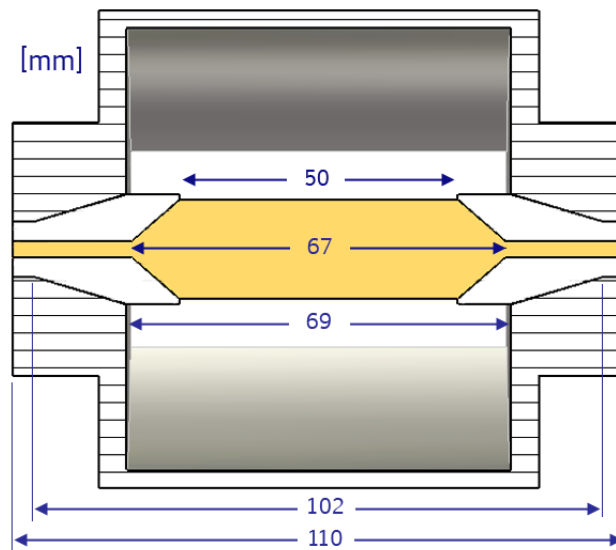


Fig. 10. Front sectional view of the jig for optimized bandwidth.

Actually, we can get an unexpected better bandwidth if we looked at the problem from the following physical sense: The voltage standing wave ratio is affected by transitions in characteristic impedances more than the values of impedances themselves, therefore, tapering improves VSWR.

Before going ahead, let us check the regions at which the modified jig suffers from high transitions. To do so the characteristic impedance at the full width of the jig must be evaluated as shown in Fig. 9, which is an advance to the work achieved in [12]. Fig. 9 shows that a big transition in characteristic impedance of about 60Ω occurs at the inner strip of the jig. Altering the shape of the copper rod and Teflon with conserving the rode diameter using the EM-Model leads to the optimized configuration shown in Fig. 10.

Predicted VSWR from CST optimized EM-model (dash-dotted line) is plotted in Fig. 11 versus measured (solid line) and EM-model (dashed line) for fabricated prototype, and to assure the
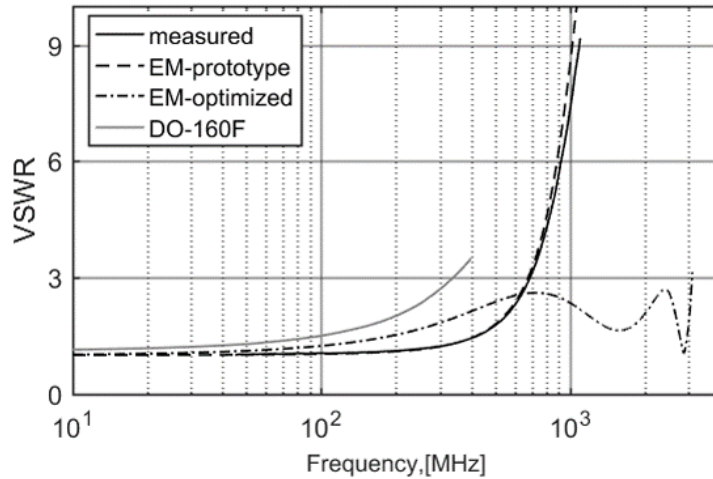
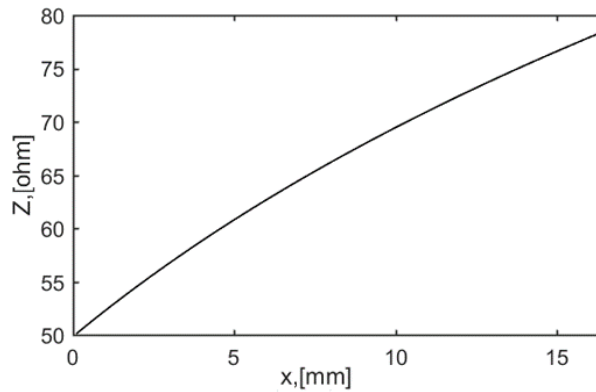Fig. 11.VSWR spectra, optimized versus fabricated CF and DO-160F standard.



Fig. 12. Characteristic impedance at the tapered region of optimized model.

compliance with regulatory standards requirements, the curve of DO-160F (solid curve) is plotted too. It can be shown that the bandwidth of the prototype can be improved up to 3GHz in respect to regulatory standards requirements with conserving the probe's clamping window. Evaluated characteristic impedance at tapered region of optimized model is shown in Fig. 12, which reflects a contrary increased impedance instead of the decreased one illustrated in Fig. 9. This proves that the tapered region plays an important role in improving the jig high frequency performance.

The optimized jig wasn't fabricated due to the limitation in bandwidth of BCI probe that is in the disposal of the authors.

## IV. PARAMETRIC STUDY OF BCI PROBE

### A. *Effect of Slot Distance*

The effect of changing the slot distance on the reflection coefficient and input impedance was studied in [13]. The effect of changing the slot distance on measured IL is shown in Fig. 13 for Wurth prototype, and Fig. 14 for Fair-Rite prototype, they show that increasing the slot distance improves the high frequency response of the probe.
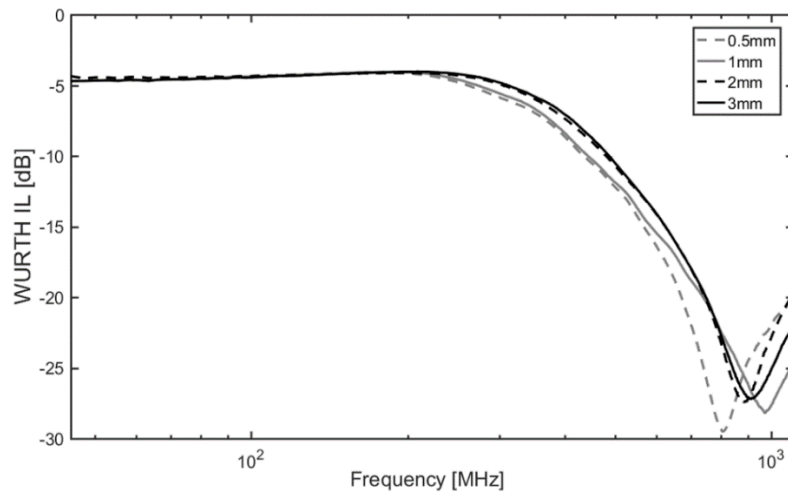
Fig. 13. Effect of changing the slot distance (d in Fig. 2) on the IL of Wurth prototype.
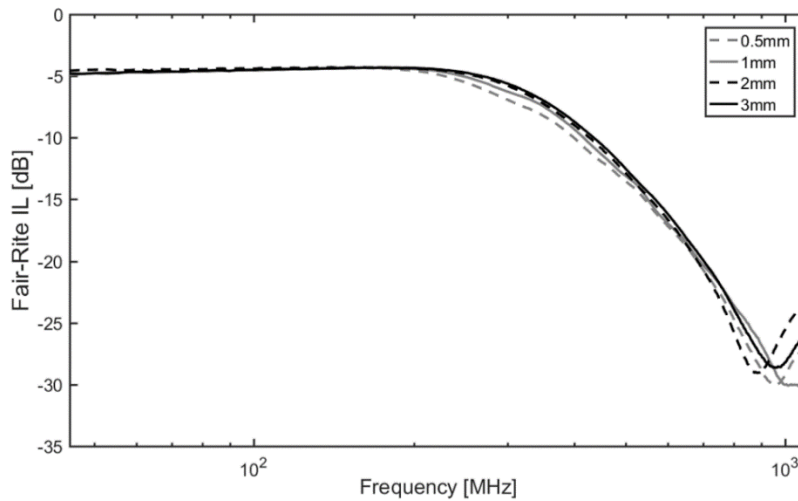


Fig. 14. Effect of changing the slot distance (d in Fig. 2) on the IL of Fair-Rite prototype.

### B.   *Effect of Shield to Core Spacing*

The space distances between the core and the shield were increased to show its effect on measured IL, in which S1 and S3 were increased by one millimeter, while S2 increased by just 0.5mm. The result of implementing these changee is shown in Fig. 15 for WURTH prototype, and Fig. 16 for Fair-Rite. The hybrid model developed in [13] is the only way to interpret the decrease resultant in the high frequency response, this shows the effectiveness of the proposed model. The explicit model, derived in [14], don't that the inter winding capacitance into consideration, therefore it can't interpret its effect.
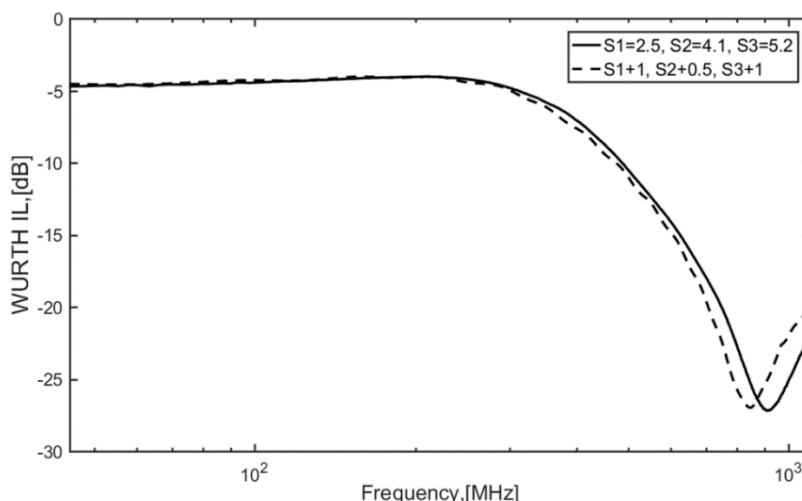
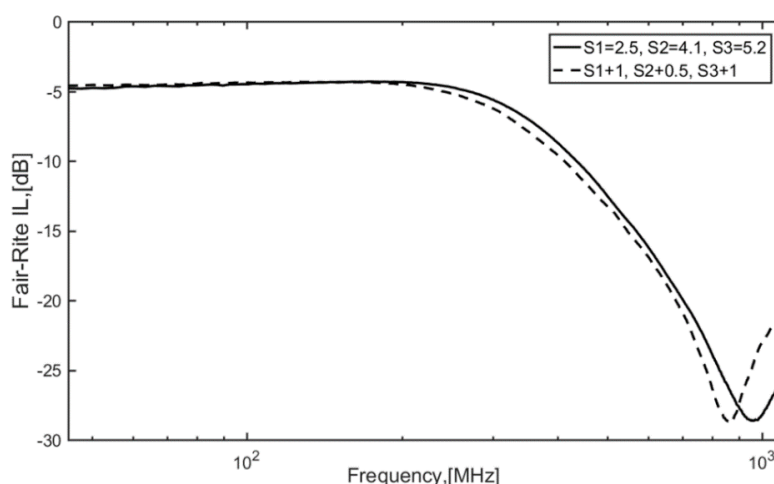Fig. 15. Effect of changing the space distance between the core and the shield on the IL of Wurth prototype (d=3mm).



Fig. 16. Effect of changing the space distance between the core and the shield on the IL of Fair-rite prototype (d=3mm).

## C.   *Effect of the Probe-Shield Spacing*

The inner rod of the jig has a radius of 9 mm (r in Fig. 8), while the inner radius of the shield has a radius of 10 mm (the inner cylinder of the shield shown in Fig. 4(b)), this lets a spacing of 1mm between the shield and the rod. To show its effect on resulted IL, this spacing was increased by 0.5 mm so that the new inner radius of the shield becomes 10.5 mm. The result shown in Fig. 17, for Fair-Rite prototype, says that the insertion loss improves by increasing the space distance between the shield of the probe and rod of the jig. Increasing this distance has the effect of decreasing the capacitor $C_2$ in the model proposed on [13]. The dependence of the probe IL on the jig imposes a question about the correctness of using the measured IL in determining the working bandwidth of the BCI-probe as proposed by DO-160F [1] and MIL-STD-461E [6], because the result would depends on the construction of the jig.
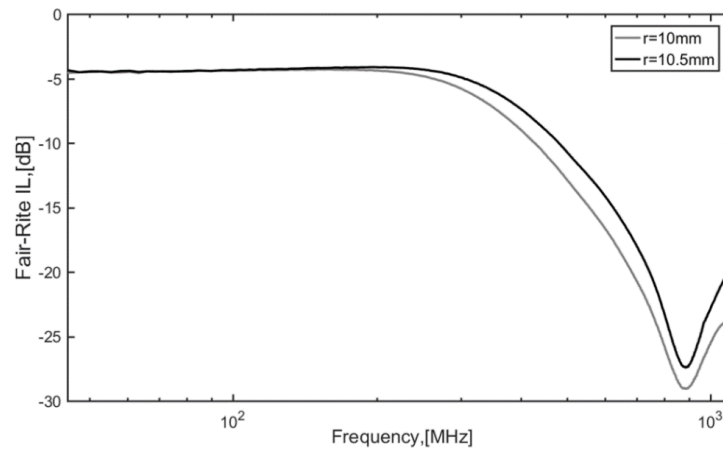
Fig. 17. Effect of changing the space distance between the shield and the rod of the jig on the IL of
Fair-rite prototype (d=2mm).



Fig. 18. The probe shield after cutting the most of its inner part.

### D. *Effect of the Shield Inner Surface*

Another way to decrease the capacitor C2 resultant between the probe and the jig is carried out by decreasing the common surface between the inner shield of the probe and the rod of the jig, therefore, most of the inner shield of the probe was cut as shown in Fig. 18. The effect of implementing this change on measured IL is shown in Fig. 19, it shows a big improvement (about 200MHz at -10dB) in the probe working bandwidth. The effect of proposed change on the probe reflection coefficient when the it is not clamped into the jig is shown in Fig. 20. This illustrates the effect of capacitive coupling between the probe shield and the jig on the probe performance.

### E. *Fair-Rite Versus Wurth*

For comparing the ferrite materials, the insertion loss of the two prototypes is measured in the same conditions at the full band, therefore, A Rohde & Schwarz VNA is used to achieve this test. The result of comparison is shown in Fig. 21, it shows that Wurth prototype has a little better performance at
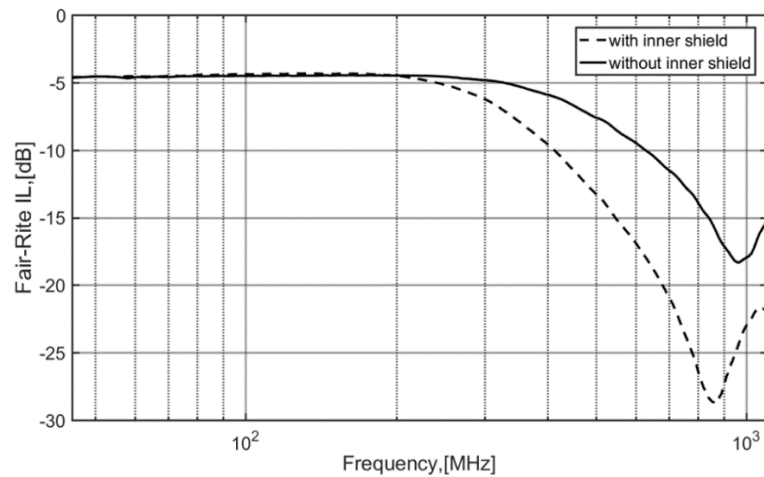
Fig. 19. Effect of cutting the inner shield of the probe on  measured IL for Fair-Rite prototype.
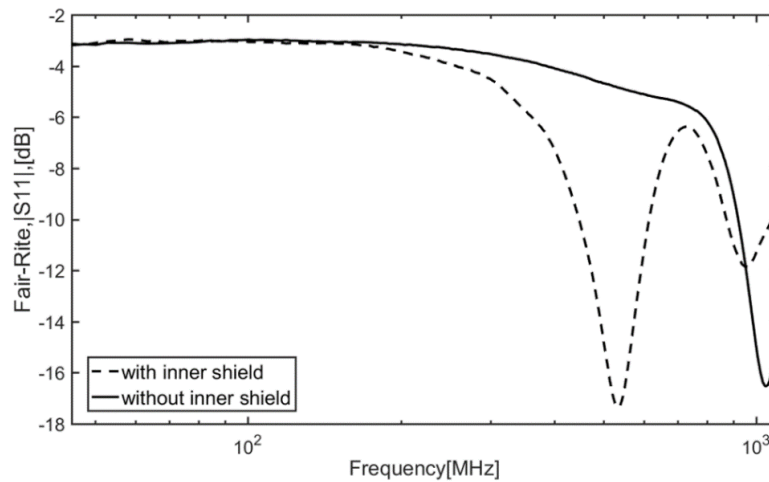


Fig. 20. Effect of cancelling the most of the probe inner shield on its measured reflection coefficient.

high frequencies, but Fair-Rite prototype surpasses it in its working bandwidth which cover a wider band of frequencies.

*F.  Fair-Rite Versus F-130a*

A comparison between Fair-Rite prototype and the probe model F-130A [15], via IL, is done as shown in Fig. 22. It shows that F-130A has a little better characteristic at high frequencies than the prototype, while the prototype has a better performance at low frequencies. The high frequency performance of the prototype can be improved at the final version to reach that of F-130A, this imply to implement a new shield with taking into account this study, the prototype was altered for a negative performance in some stages to achieve the needed study, and these changes are not reversible, thus, the final result shown here is not the best result.
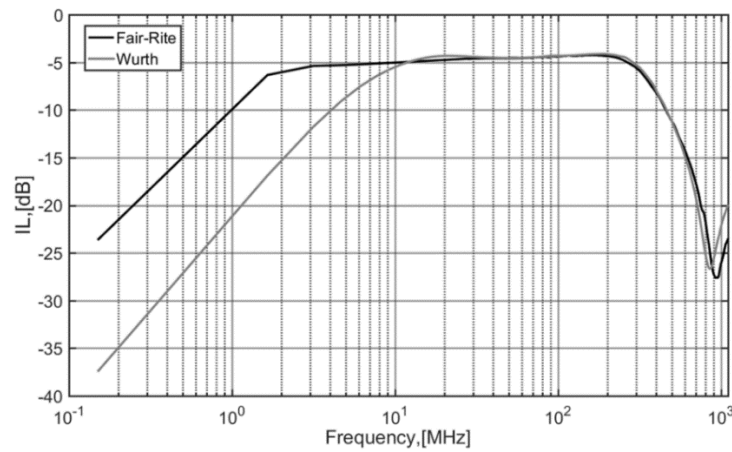
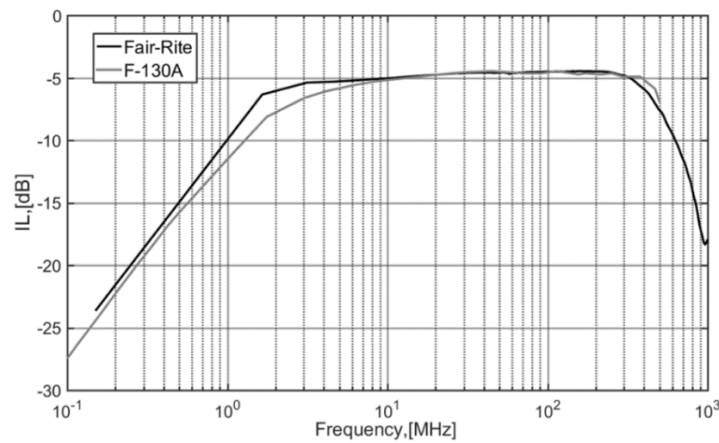Fig. 21. Fair-Rite prototype versus WURTH prototype.



Fig. 22. Fair-Rite prototype versus probe model F-130A.

### G. Fair-Rite Versus Standards

Comparing the developed Fair-Rite prototype with DO-160F [1] and MIL-STD [6] requirements helps in estimating the range of frequencies at which the proposed probe could be used. The result of comparison shown in Fig. 23, indicates that Fair-Rite prototype can be used in the limit frequencies from 600kHz up to 600MHz.

### H. Uncertainty

To evaluate the precision of measurements and its repeatability. Estimating the uncertainty of measured insertion loss is carried out. Therefore, ten measurements for IL are recorded. Calibration of the VNA is done in the band 45-1100 MHz with 201 sample frequency. Using MATLAB software, the mean and standard deviation values of IL are calculated first at each sample frequency, then, the standard deviation of the mean values or uncertainties at that frequencies are calculated. The result of
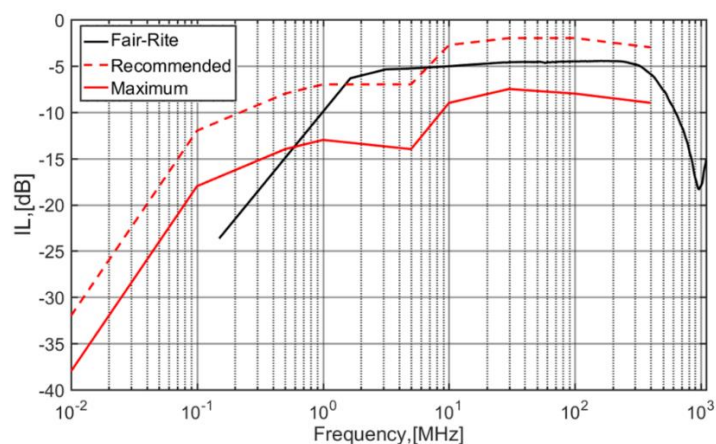
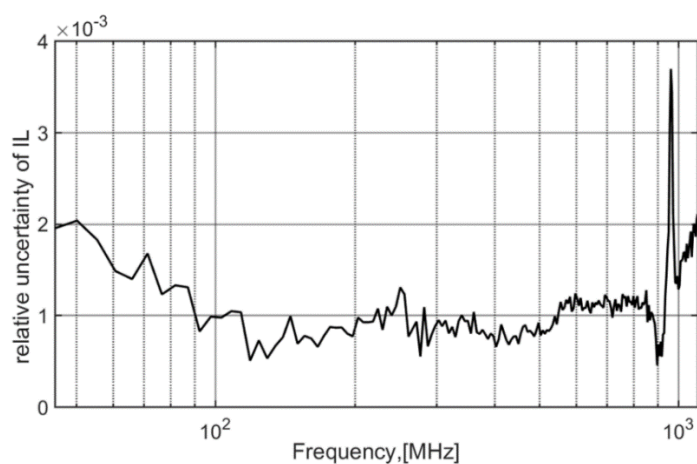Fig. 23. Fair-Rite prototype versus DO-160F and MIL-STD.



Fig. 24. measures relative standard uncertainty spectra of IL at 201 sample

Fig. 24, shows that the device has a maximum relative uncertainty in measured IL of about 0.002 up to 900 MHz within the measuring frequencies.

## V.  CONCLUSION

A calibration jig with rounded shield was implemented and optimized, the prototype showed a good characteristic, and the optimization is carried out on the rod shape with conserving the clamping window. The result of optimization showed more than four times improvement in the jig bandwidth, via its predicted VSWR. Two ferrite materials were used in implementing two prototypes of BCI-probe, Fair-Rite core showed better characteristics than WURTH at low frequencies. Increasing the slot distance showed to improve measured insertion loss. The separating distance between the core and the shield showed that increasing it affects negatively on measured IL. It was shown that, the

capacitive coupling between the injection probe and the jig can be controlled by the space distance between the inner shield of the probe and the rod of the jig, and by the common surface between them. Increasing the separating distance, by increasing the inner radius of the probe or decreasing the radius of jig rod, can apparently improve the probe measured insertion loss. Widening the slot existed in the shield's inner surface has the same effect of improving measured insertion loss.

## REFERENCES

[1]  RTCA/DO-160F - "Environmental conditions and test procedures for airborne equipment," 2007.

[2]  Electromagnetic compatibility (EMC) -Part4–6: Testing and measurement techniques-Immunity to conducted disturbances, induced by radio-frequency fields, IEC Standard 61000-4-6, May 2006.

[3]  ISO Standard 11451-4: Road Vehicles-Vehicle test methods for electrical disturbances from narrowband radiatedelectromagnetic energy-Part4: Bulk Current Injection (BCI), June, 2006.

[4]   ISO Standard 11452-4: Road Vehicles- Component Test Methods for Electrical Disturbances from Narrowband Radiated Electromagnetic Energy-Part4: Harness excitation methods, Dec.2011.

[5]  IEC 62132-3, Ed.1: Integrated Circuit Measurements of Electromagnetic Immunity 150kHz to 1GHz, Part 3: Bulk Current Injection (BCI) Method, 2007.

[6]  Department of Defense Interface Standard, "Requirements for the Control of Electromagnetic Interference Characteristics of Subsystems and Equipment", MIL-STD-461E, Aug. 20, 1999.

[7]  Fischer Custom Communications BCI Brochure, Fischer Custom Communications, Inc.

[8]  H. Sekiguchi, T. Funaki, "Proposal for Measurement Method of Transfer Impedance of Current Probe," *IEEE Trans. EMC*, vol. 56, no. 4, pp. 871-877, Aug. 2014.

[9]  L. W. Ma, C. Yu, "Correlation between Transfer Impedance and Insertion Loss of Current Probes," *IEEE EMC Magazine*, vol. 3, no. 2, pp. 51-55, 2nd Quarter 2014.

[10] F. Grassi, S.A. Pignari "Characterization of the Bulk Current of Injection Calibration-jig for the Probe-Model Extraction," *2010 IEEE International Symposium on EMC*, Fort Lauderdale, FL, pp. 344-347 , July 2010.

[11] N. Toscani, F. Grassi, G. Spadacini, S.A. Pignari, "Circuit and Electromagnetic Modeling of Bulk Current Injection Test Setups Involving Complex Wiring Harnesses," *IEEE Trans. EMC*, vol. 60, no. 6, pp. 1752-1760, Dec. 2018.

[12] I. M. Mashriki, S. M. J. Razavi, S. H. M. Armaki, "Electromagnetic and circuit modelling of a modified design of bulk current injection probe calibration jig," *IET Science, Measurement & Technology, in IET Science*, vol. 14, no. 9, pp. 715-721, Nov. 2020.

[13] I. M. Mashriki, S. M. J. Razavi, S. H. M. Armaki, "Hybrid Model for Bulk Current Injection Probe," *Journal of Communication Engineering,* vol. 8, no. 2, pp. 277-289, July-Dec. 2019.

[14] I. M. Mashriki, S. M. J. Razavi, S. H. M. Armaki, "Analyzing the Resonance Resultant from the Capacitive Effects in Bulk Current Injection Probe," *Radioengineering*, vol. 29, pp. 109-116, April 2020.

[15] F. Grassi, F. Marliani, S.A. Pignari "Circuit Modeling of Injection Probes For Bulk Current Injection," *IEEE Trans. Electromagnetic, Compatibility.,* vol. 49, no. 3, pp. 563-576, Aug. 2007.